Relativistic Mean-Field Hadronic Models under Nuclear Matter Constraints

Débora Peres Menezes - Universidade Federal de Santa Catarina - Florianópolis - Brazil

Brazil - JINR Forum - June, 2015

Author's list:

- **Mariana Dutra** - Departamento de Física e Matemática - ICT, Universidade Federal Fluminense, 28895-532 Rio das Ostras, RJ, Brazil

- **Odilon Lourenço** - Departamento de Ciências da Natureza, Matemática e Educação, CCA, Universidade Federal de São Carlos, 13600-970 Araras, SP, Brazil

- **Sidney S. Avancini** - Depto de Física - CFM - Universidade Federal de Santa Catarina, Florianópolis - SC - CP. 476 - CEP 88.040 - 900 - Brazil

- **Brett V. Carlson** - Departamento de Física, Instituto Tecnológico de Aeronáutica, CTA, 12228-900 São José dos Campos, SP, Brazil

- **Antonio Delfino** - Departamento de Física - Universidade Federal Fluminense, Av. Litorânea s/n, 24210-150 Boa Viagem, Niterói, RJ, Brazil

- **Contança Providência** - Centro de Física Computacional, Department of Physics, University of Coimbra, P-3004-516 Coimbra, Portugal

- **Stefan Typel** - GSI Helmholtzzentrum für Schwerionenforschung GmbH, Theorie, Planckstrasse 1,D-64291 Darmstadt, Germany

- **Jirina R. Stone** - Oxford Physics, University of Oxford, OX1 3PU Oxford, United Kingdom; Department of Physics and Astronomy, University of Tennessee, Knoxville, Tennessee 37996, USA

- **D.P.M.**

Motivation

- EoS are essential for modeling compact astrophysical objects such as neutron stars, core-collapse supernovae and related phenomena including the creation of chemical elements in the Universe.

- No realistic and quantitative description of infinite hadronic matter and nuclei from first principles is available at present. Hence, too many models have been developed.

- It is important to determine the most realistic parameter sets and to use them consistently.

- Recently a set of constraints on properties of nuclear matter was formed and the performance of **240 non-relativistic Skyrme** parameterizations was assessed, in describing nuclear matter up to about 3 times nuclear saturation density. **16** were approved.

- We have also examined **263 Relativistic mean-field (RMF) models** in a comparable approach.

- **Three** different sets of constraints related to **symmetric nuclear matter, pure neutron matter, symmetry energy, and its derivatives were used**:
  - **SET1** -the same as used in assessing the Skyrme parameterizations. (M. Dutra, O. Lourenço, J. S. Sá Martins, A. Delfino, J. R. Stone, and P. D. Stevenson, Phys. Rev. C **85**, 035201 (2012))
  - **SET2a and SET2b (more restricitive)**, were more suitable for analysis of RMF and included, up-to-date theoretical, experimental and empirical information.

Non-linear models

$$\mathcal{L}_{\text{NL}} = \mathcal{L}_{\text{nm}} + \mathcal{L}_\sigma + \mathcal{L}_\omega + \mathcal{L}_\rho + \mathcal{L}_\delta + \mathcal{L}_{\sigma\omega\rho}, \tag{1}$$

$$\mathcal{L}_{\text{nm}} = \overline{\psi}(i\gamma^\mu\partial_\mu - M)\psi + g_\sigma\sigma\overline{\psi}\psi - g_\omega\overline{\psi}\gamma^\mu\omega_\mu\psi - \frac{g_\rho}{2}\overline{\psi}\gamma^\mu\vec{\rho}_\mu\vec{\tau}\psi + g_\delta\overline{\psi}\vec{\delta}\vec{\tau}\psi, \tag{2}$$

$$\mathcal{L}_\sigma = \frac{1}{2}(\partial^\mu\sigma\partial_\mu\sigma - m_\sigma^2\sigma^2) - \frac{A}{3}\sigma^3 - \frac{B}{4}\sigma^4, \tag{3}$$

$$\mathcal{L}_\omega = -\frac{1}{4}F^{\mu\nu}F_{\mu\nu} + \frac{1}{2}m_\omega^2\omega_\mu\omega^\mu + \frac{C}{4}(g_\omega^2\omega_\mu\omega^\mu)^2, \tag{4}$$

$$\mathcal{L}_\rho = -\frac{1}{4}\vec{B}^{\mu\nu}\vec{B}_{\mu\nu} + \frac{1}{2}m_\rho^2\vec{\rho}_\mu\vec{\rho}^\mu, \tag{5}$$

$$\mathcal{L}_\delta = \frac{1}{2}(\partial^\mu\vec{\delta}\partial_\mu\vec{\delta} - m_\delta^2\vec{\delta}^2), \tag{6}$$

$$\mathcal{L}_{\sigma\omega\rho} = g_\sigma g_\omega^2\sigma\omega_\mu\omega^\mu\left(\alpha_1 + \frac{1}{2}\alpha_1{}'g_\sigma\sigma\right) + g_\sigma g_\rho^2\sigma\vec{\rho}_\mu\vec{\rho}^\mu\left(\alpha_2 + \frac{1}{2}\alpha_2{}'g_\sigma\sigma\right)$$
$$+ \frac{1}{2}\alpha_3{}'g_\omega^2 g_\rho^2\omega_\mu\omega^\mu\vec{\rho}_\mu\vec{\rho}^\mu. \tag{7}$$

Mean-field approximation (the meson fields are treated as classical fields):

$$\sigma \to \langle\sigma\rangle \equiv \sigma, \quad \omega_\mu \to \langle\omega_\mu\rangle \equiv \omega_0, \quad \vec{\rho}_\mu \to \langle\vec{\rho}_\mu\rangle \equiv \bar{\rho}_{0(3)}, \quad \vec{\delta} \to <\vec{\delta}> \equiv \delta_{(3)}, \tag{8}$$

Euler-Lagrange equations $\to$ equations of motion (translational and rotational invariance) $\to$ energy-momentum tensor $\to$ EoS

Dirac equation $\to$ **vector and scalar potentials**:

$$V_{\tau\,\mathrm{NL}} = g_\omega \omega_0 + \frac{g_\rho}{2}\bar{\rho}_{0(3)}\tau_3 \tag{9}$$

$$S_{\tau\,\mathrm{NL}} = -g_\sigma \sigma - g_\delta \delta_{(3)}\tau_3, \tag{10}$$

$M^*_\tau = M + S_{\tau\,\mathrm{NL}} \to$

$$M^*_p = M - g_\sigma\sigma - g_\delta\delta_{(3)} \qquad \text{and} \qquad M^*_n = M - g_\sigma\sigma + g_\delta\delta_{(3)}. \tag{11}$$

- **type 1** (linear finite range models): $A = B = C = \alpha_1 = \alpha_2 = \alpha'_1 = \alpha'_2 = \alpha'_3 = g_\delta = 0$ (linear Walecka model)

- **type 2** ($\sigma^3 + \sigma^4$ models): $C = \alpha_1 = \alpha_2 = \alpha'_1 = \alpha'_2 = \alpha'_3 = g_\delta = 0$. (Boguta-Bodmer model)

- **type 3** ($\sigma^3 + \sigma^4 + \omega_0^4$ models): $\alpha_1 = \alpha_2 = \alpha'_1 = \alpha'_2 = \alpha'_3 = g_\delta = 0$. (include a quartic self-interaction in the ω field)

- **type 4** ($\sigma^3 + \sigma^4 + \omega_0^4$ + cross terms models): $g_\delta = 0$ and at least one of the coupling constants, α_1, α_2, α'_1, α'_2, or α'_3 is different from zero.

Density dependent models

$$g_\sigma \to \Gamma_\sigma(\rho), \quad g_\omega \to \Gamma_\omega(\rho), \quad g_\rho \to \Gamma_\rho(\rho) \quad \text{and} \quad g_\delta \to \Gamma_\delta(\rho) \tag{12}$$

$$\begin{aligned}
\mathcal{L}_{\mathrm{DD}} &= \overline{\psi}(i\gamma^\mu\partial_\mu - M)\psi + \Gamma_\sigma(\rho)\sigma\overline{\psi}\psi - \Gamma_\omega(\rho)\overline{\psi}\gamma^\mu\omega_\mu\psi - \frac{\Gamma_\rho(\rho)}{2}\overline{\psi}\gamma^\mu\vec{\rho}_\mu\vec{\tau}\psi \\
&+ \frac{1}{2}(\partial^\mu\sigma\partial_\mu\sigma - m_\sigma^2\sigma^2) - \frac{1}{4}F^{\mu\nu}F_{\mu\nu} + \frac{1}{2}m_\omega^2\omega_\mu\omega^\mu - \frac{1}{4}\vec{B}^{\mu\nu}\vec{B}_{\mu\nu} + \frac{1}{2}m_\rho^2\vec{\rho}_\mu\vec{\rho}^\mu \\
&+ \Gamma_\delta(\rho)\overline{\psi}\vec{\delta}\vec{\tau}\psi + \frac{1}{2}(\partial^\mu\vec{\delta}\partial_\mu\vec{\delta} - m_\delta^2\vec{\delta}^2),
\end{aligned} \tag{13}$$

$$\Gamma_i(\rho) = \Gamma_i(\rho_0)f_i(x), \quad f_i(x) = a_i\frac{1+b_i(x+d_i)^2}{1+c_i(x+d_i)^2} \quad i = \sigma, \omega, \tag{14}$$

$$\Gamma_\rho(\rho) = \Gamma_\rho(\rho_0)e^{-a(x-1)}, \quad x = \rho/\rho_0. \tag{15}$$

the GDFM model:

$$\Gamma_i(\rho) = a_i + (b_i + d_i x^3) e^{-c_i x}, \quad i = \sigma, \omega, \rho, \delta \tag{16}$$

and a correction to the coupling parameter for the meson ω :

$$\Gamma_{\mathrm{cor}}(\rho) = \Gamma_\omega(\rho) - a_{\mathrm{cor}} e^{-\left(\frac{\rho-\rho_0}{b_{\mathrm{cor}}}\right)^2}. \tag{17}$$

DDHδ parameterization: same coupling parameters as in Eq. (14) for σ and ω

$$f_i(x) = a_i e^{-b_i(x-1)} - c_i(x - d_i), \quad i = \rho, \delta \tag{18}$$

$$V_{\tau\,\mathrm{DD}} \;=\; \Gamma_\omega(\rho)\omega_0 + \frac{\Gamma_\rho(\rho)}{2}\bar{\rho}_{0(3)}\tau_3 + \Sigma_R(\rho), \tag{19}$$

$$\Sigma_R(\rho) = \frac{\partial\Gamma_\omega}{\partial\rho}\omega_0\rho + \frac{1}{2}\frac{\partial\Gamma_\rho}{\partial\rho}\bar{\rho}_{0(3)}\rho_3 - \frac{\partial\Gamma_\sigma}{\partial\rho}\sigma\rho_s - \frac{\partial\Gamma_\delta}{\partial\rho}\delta_{(3)}\rho_{s3} \tag{20}$$

- **type 5** (density dependent models): parameterizations obtained from Eq. (13) in which $\Gamma_\delta = 0$.

Nonlinear point-coupling models

$$
\begin{aligned}
\mathcal{L}_{\mathrm{NLPC}} &= \overline{\psi}(i\gamma^\mu\partial_\mu - M)\psi - \frac{\alpha_s}{2}(\overline{\psi}\psi)^2 - \frac{\beta_s}{3}(\overline{\psi}\psi)^3 - \frac{\gamma_s}{4}(\overline{\psi}\psi)^4 \\
&- \frac{\alpha_{\mathrm{V}}}{2}(\overline{\psi}\gamma^\mu\psi)^2 - \frac{\gamma_{\mathrm{V}}}{4}(\overline{\psi}\gamma^\mu\psi)^4 - \frac{\alpha_{\mathrm{TV}}}{2}(\overline{\psi}\gamma^\mu\vec{\tau}\psi)^2 - \frac{\gamma_{\mathrm{TV}}}{4}(\overline{\psi}\gamma^\mu\vec{\tau}\psi)^4 \quad (21) \\
&- \frac{\alpha_{\mathrm{TS}}}{2}(\overline{\psi}\vec{\tau}\psi)^2 + \left[\eta_1 + \eta_2(\overline{\psi}\psi)\right](\overline{\psi}\psi)(\overline{\psi}\gamma^\mu\psi)^2 - \eta_3(\overline{\psi}\psi)(\overline{\psi}\gamma^\mu\vec{\tau}\psi)^2.
\end{aligned}
$$

$$
\begin{aligned}
V_{\tau\,\mathrm{NLPC}} &= \alpha_{\mathrm{V}}\rho + \alpha_{\mathrm{TV}}\rho_3\tau_3 + \gamma_{\mathrm{V}}\rho^3 + \gamma_{\mathrm{TV}}\rho_3^3\tau_3 + 2(\eta_1 + \eta_2\rho_s)\rho_s\rho + 2\eta_3\rho_s\rho_3\tau_3, \\
S_{\tau\,\mathrm{NLPC}} &= \alpha_s\rho_s + \beta_s\rho_s^2 + \gamma_s\rho_s^3 + \eta_1\rho^2 + 2\eta_2\rho_s\rho^2 + \eta_3\rho_3^2 + \alpha_{\mathrm{TS}}\rho_{s3}\tau_3, \qquad (22)
\end{aligned}
$$

$$
M_p^* = M + \alpha_s\rho_s + \beta_s\rho_s^2 + \gamma_s\rho_s^3 + \eta_1\rho^2 + 2\eta_2\rho_s\rho^2 + \eta_3\rho_3^2 + \alpha_{\mathrm{TS}}\rho_{s3}, \quad (23)
$$

$$
M_n^* = M + \alpha_s\rho_s + \beta_s\rho_s^2 + \gamma_s\rho_s^3 + \eta_1\rho^2 + 2\eta_2\rho_s\rho^2 + \eta_3\rho_3^2 - \alpha_{\mathrm{TS}}\rho_{s3}. \quad (24)
$$

- **type 6** (point-coupling models): parameterizations of the model described by Eq. (22) in which $\alpha_{\mathsf{TS}} = 0$.

- **type 7** (delta meson models): parameterizations of finite range models presenting the meson δ, i.e., models in which $g_\delta \neq 0$.

Nuclear bulk matter quantities

$$\mathcal{S}(\rho) = \frac{1}{8}\frac{\partial^2(\mathcal{E}/\rho)}{\partial y^2}\bigg|_{\rho,y=1/2}, \quad \text{(symmetry energy)} \tag{25}$$

$$K_0 = 9\left(\frac{\partial P}{\partial \rho}\right)_{\rho=\rho_0,y=1/2}, \quad \text{(incompressibility)} \tag{26}$$

$$Q_0 = 27\rho_0^3\frac{\partial^3(\mathcal{E}/\rho)}{\partial \rho^3}\bigg|_{\rho=\rho_0,y=1/2}, \quad \text{(skewness coefficient)} \tag{27}$$

$$J = \mathcal{S}(\rho_0), \quad \text{(symmetry energy at } \rho=\rho_0) \tag{28}$$

$$L_0 = 3\rho_0\left(\frac{\partial \mathcal{S}}{\partial \rho}\right)_{\rho=\rho_0}, \quad \text{(slope of } \mathcal{S}) \tag{29}$$

$$K^0_{\rm sym} = 9\rho_0^2\left(\frac{\partial^2 \mathcal{S}}{\partial \rho^2}\right)_{\rho=\rho_0}, \quad \text{(curvature of } \mathcal{S}) \tag{30}$$

$$Q^0_{\rm sym} = 27\rho_0^3\left(\frac{\partial^3 \mathcal{S}}{\partial \rho^3}\right)_{\rho=\rho_0}, \quad \text{(skewness of } \mathcal{S}) \tag{31}$$

$$K^0_{\tau,\rm v} = \left(K^0_{\rm sym} - 6L_0 - \frac{Q_0}{K_0}L_0\right). \quad \text{(vol part isospin incompressibility)} \tag{32}$$

Constraints - SET 1

SET1 - 11 macroscopic constraints, range of their experimental/empirical values, density region in which they are valid and the corresponding range obtained using the approved RMF models (CRMF).

	Quantity	Density Region	Range of constraint (exp/emp)	Range of constraint from CRMF
SM1	K_0	ρ_0 (fm^{-3})	200-260 MeV	271.0 MeV
SM2	$K' = -Q_0$	ρ_0 (fm^{-3})	200-1200 MeV	733.6 MeV
SM3	$P(\rho)$	$2 < \frac{\rho}{\rho_0} < 4.6$	Band Region	see Fig.
SM4	$P(\rho)$	$1.2 < \frac{\rho}{\rho_0} < 2.2$	Band Region	see Fig.
PNM1	$\mathcal{E}_{PNM}/\rho$	$0.017 < \frac{\rho}{\rho_o} < 0.108$	Band Region	see Fig.
PNM2	$P(\rho)$	$2 < \frac{\rho}{\rho_0} < 4.6$	Band Region	see Fig.
MIX1	J	ρ_0 (fm^{-3})	30-35 MeV	33.8-34.0 MeV
MIX2	L_0	ρ_0 (fm^{-3})	40-76 MeV	70.9-73.9 MeV
MIX3	$K^0_{\tau,V}$	ρ_0 (fm^{-3})	-760/-372 MeV	-388.5/-388.4 Me
MIX4	$\frac{\mathcal{S}(\rho_0/2)}{J}$	ρ_0 (fm^{-3})	0.57-0.86	0.58
MIX5	$\frac{3P_{PNM}}{L_0\rho_0}$	ρ_0 (fm^{-3})	0.90-1.10	1.05-1.06

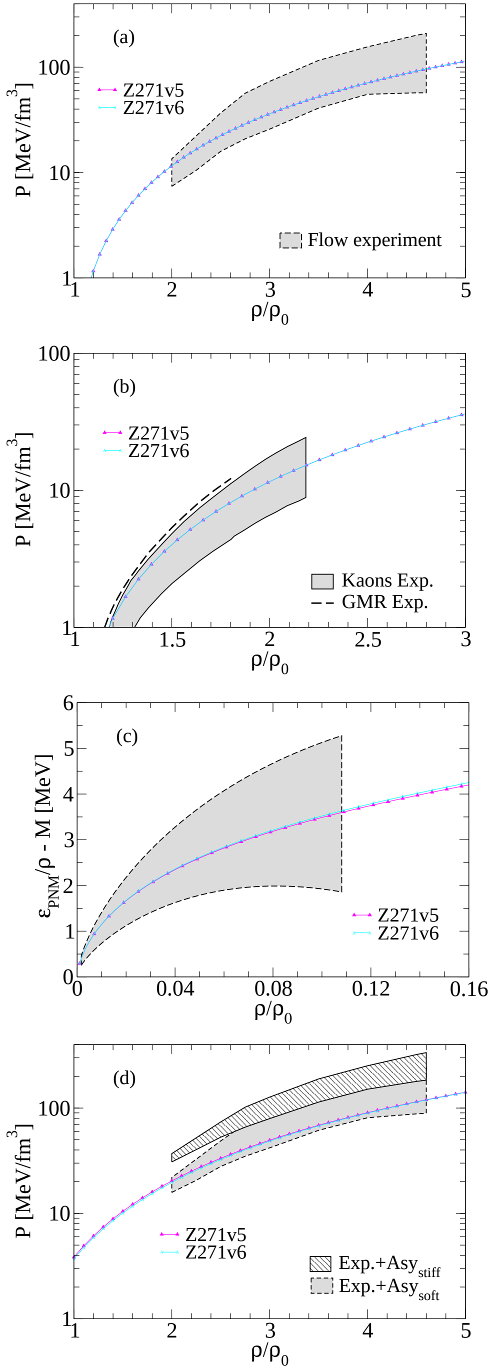

SM3 - symmetric matter

SM4 - Prog. Part. Nucl. Phys. **62**, 427 (2009)

PNM1 - Phys. Rev. C **85**, 035201 (2012)

PNM2 - pure neutron matter

A model is considered approved if its deviation obeys $|\text{Dev}| \leq 1$.

$$\text{Dev} = \frac{Q_{\text{mod}} - Q_{\text{const}}}{\Delta}, \tag{33}$$

Q_{mod} is value of the quantity calculated in the model, Q_{const} the central value of the related constraint, and Δ the error related to Q_{const}.

For the MIX1, MIX3 and MIX4 constraints, we define $Q_{\text{const}} = (x_2 + x_1)/2$ and the error $\Delta = x_2 - Q_{\text{const}} = Q_{\text{const}} - x_1$, since they are given in the form of $x_1 \leq X \leq x_2$.

A graphic constraint is satisfied if the model is inside the corresponding band in 95% or more of the density region.

None of the models satisfies all constraints simultaneously.

List of parametrizations that **fail in only one** constraint of SET1:

Model	Model value (MeV)	Deviation
SM1 not satisfied: $200 \leq K_0 \leq 260$ MeV		
Z271v5 (type 4)	271.00	1.37
Z271v6 (type 4)	271.00	1.37
MIX3 not satisfied: $-760 \leq K_{\tau,\mathrm{v}}^{0} \leq -372$ MeV		
BSR15 (type 4)	-252.54	1.62
BSR16 (type 4)	-258.75	1.58
FSUGold (type 4)	-276.07	1.49
FSUGZ06 (type 4)	-259.47	1.58
FSUGold4 (type 4)	-205.59	1.86
FSU-III (type 4)	-341.03	1.16
FSU-IV (type 4)	-210.68	1.83
TW99 (type 5)	-332.32	1.20
DD-F (type 5)	-285.54	1.45
DD-MEδ (type 7)	-258.28	1.59

Constraints - SET2a and SET2b

Updated constraints: SM1, SM3a, SM3b, MIX1a, MIX1b, MIX2a, MIX2b and MIX3.
SM4, PNM1 and MIX4 constraints are the same as in SET1.
SM2, PNM2 and MIX5 constraints were removed.

	Quantity	Density Region	Range of constraint (exp/emp)	Range of constraint from CRMF
SM1	K_0	ρ_0 (fm^{-3})	190-270 MeV	225.2-232.4 MeV
SM3a		the same as SM3b plus 20% on upper limit		see Fig.
SM3b	$P(\rho)$	$2 < \frac{\rho}{\rho_0} < 5$	Band Region	see Fig.
SM4	$P(\rho)$	$1.2 < \frac{\rho}{\rho_0} < 2.2$	Band Region	see Fig.
PNM1	$\mathcal{E}_{PNM}/\rho$	$0.017 < \frac{\rho}{\rho_o} < 0.108$	Band Region	see Fig.
MIX1a	J	ρ_0 (fm^{-3})	25-35 MeV	33.2-34.2 MeV
MIX1b	J	ρ_0 (fm^{-3})	30-35 MeV	33.2-34.0 MeV
MIX2a	L_0	ρ_0 (fm^{-3})	25-115 MeV	77.9-84.8 MeV
MIX2b	L_0	ρ_0 (fm^{-3})	30-80 MeV	77.9-78.8 MeV
MIX3	$K^0_{\tau,V}$	ρ_0 (fm^{-3})	-700/-400 MeV	-421.6(a)/-414.3(b)/-382.5 MeV
MIX4	$\frac{\mathcal{S}(\rho_0/2)}{J}$	ρ_0 (fm^{-3})	$0.57 - 0.86$	$0.57(a)/0.59(b) - 0.59$

shaded areas - Science **298**, 1592 (2002)

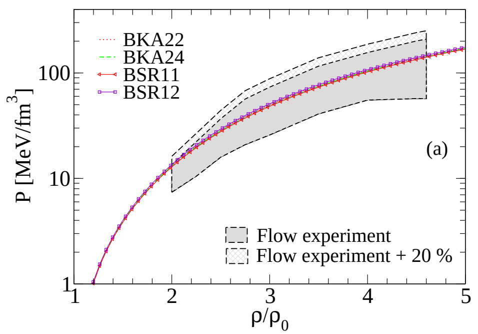

SM3

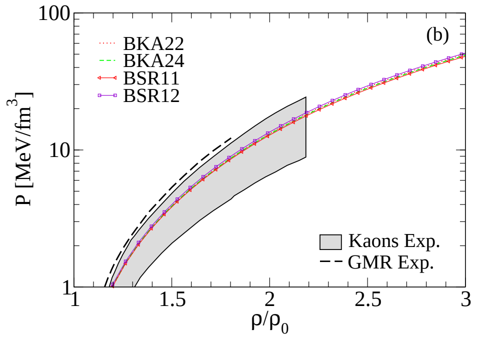

SM4

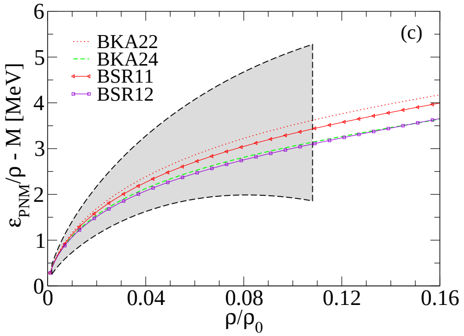

PNM1

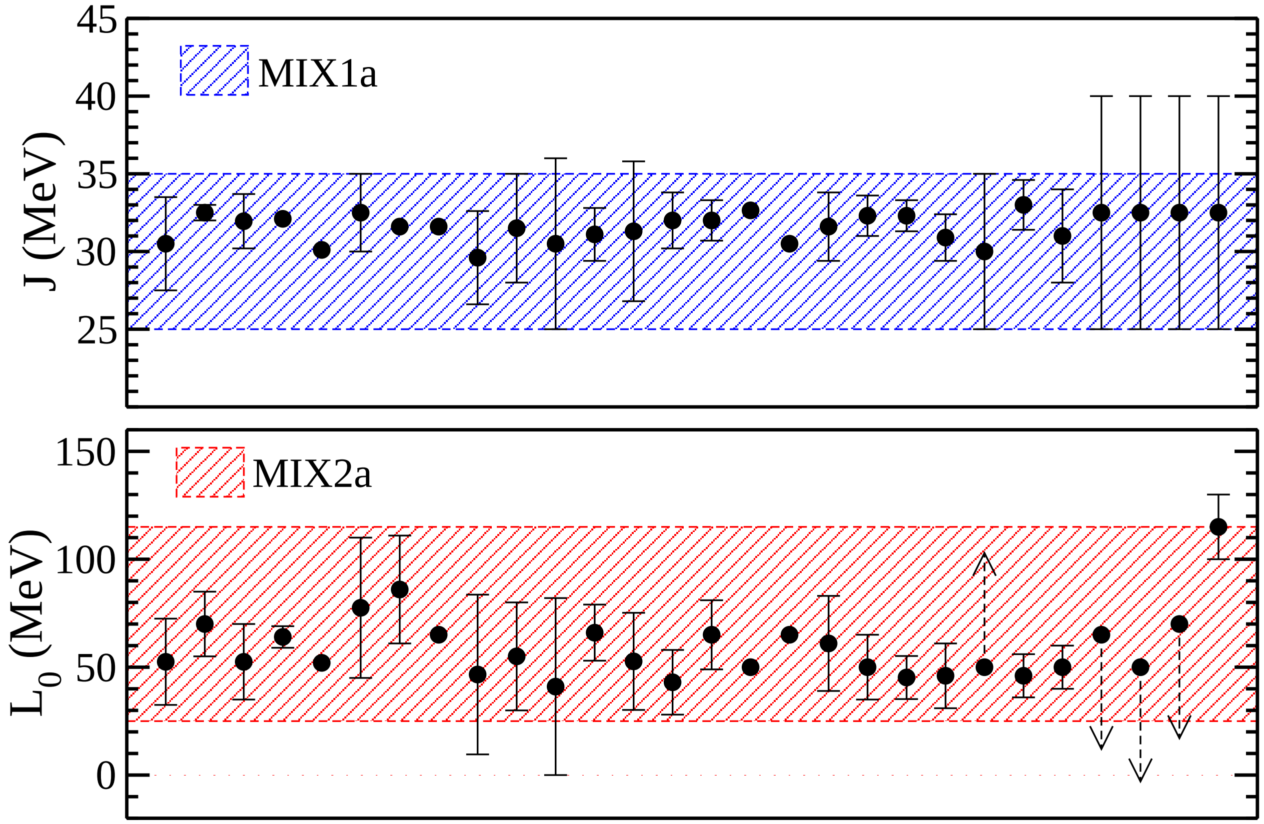

Comparison between the limits used in MIX1a and MIX2a constraints, and those from 28 **different experimental/observational data collected in B.-A. Li and X. Han, Phys. Lett. B 727, 276 (2013):** include analyses of isospin diffusion, neutron skins, pygmy dipole resonances, and decays, transverse flow, the mass-radius relation and torsional crust oscillations of neutron stars.

SET2

Constraints	SM1	SM3a	SM3b	SM4	PNM1	
Number of models	153	129	104	153	193	
Constraints	MIX1a	MIX1b	MIX2a	MIX2b	MIX3	MIX4
Number of models	174	162	216	72	96	65

SET2a: Only **2 type-4 models** satisfy all constraints: **BSR12** and **BKA24**.

SET2b: Only **1 model** satisfy all constraints: **BSR12**.

The models **FSUGold, FSUZG03, IU-FSU (type 4) and DD-MEδ (type 7)** are consistent with all constraints except MIX3, a constraint applicable in the region of saturation density. These parameter sets provide quite good global fits to binding energies, charge radii, isotopic shifts and neutron skin thicknesses

Excluding MIX3 constraint

SET2a: *25 models* are consistent with all 7 constraints: **BKA20, BKA22, BKA24, BSR8, BSR9, BSR10, BSR11, BSR12, BSR15, BSR16, BSR17, BSR18, BSR19, FSU-III, FSU-IV, FSUGold, FSUGold4, FSUGZ03, FSUGZ06, G2*, IU-FSU (***type 4***), TW99, DD-F (***type 5***), DD-MEδ, DDHδ (***type 7***)**.

48 models satisfy all but one of the constraints. In this group, 10 models fell outside the range of the constraint by less than 5%:**BSR20, FA3, Z271s2, Z271s3, Z271s4, Z271s5, Z271s6, Z271v4, Z271v5, Z271v6**.

SET2b: *22 models* are consistent with all constraints: the same models approved in SET2a, **except** for the BKA24, IU-FSU and DDHδ models.

14 models satisfy only 7 constraints, and by applying the 5% criterium, 8 more models are approved. They are the same as in the corresponding case of SET2a, **except** for the BSR20 and FA3 models. Within SET2b analysis a total of *30 models* are in the group of approved models.

Saturation properties

Model	ρ_0	E_0	K_0	m^*	K'	J	L_0	K^0_{sy}
				linear finite range models (type 1)				
H1	0.148	−15.75	546.81	0.54	−2152.62	25.93	88.38	93
				$\sigma^3 + \sigma^4$ **models (type 2)**				
CS	0.150	−16.17	187.21	0.58	292.63	40.91	131.42	136
				$\sigma^3 + \sigma^4 + \omega_0^4$ models (type 3)				
BM-A	0.179	−15.17	188.32	0.61	436.32	19.62	51.88	−18
				$\sigma^3 + \sigma^4 + \omega^4 +$ **cross terms models (type 4)**				
BKA20	0.146	−15.93	237.95	0.64	464.66	32.24	75.38	−15
				density dependent models (type 5)				
DD	0.149	−16.02	239.99	0.56	−134.65	31.64	55.98	−95
				point-coupling models (type 6)				
FA2	0.150	−16.03	287.24	0.60	812.70	33.53	99.38	−3
				delta meson models (type 7)				
DD-MEδ	0.152	−16.08	219.60	0.61	748.31	32.18	51.43	−124

Status of each RMF model: approved (+) or not (−) under SET2a and SET2b constraints.

Model	SM1	SM3a	SM3b	SM4	PNM1	MIX1a	MIX1b	MIX2a	MIX2b	MIX3
					linear finite range models					
H1	−	−	−	−	+	+	−	+	−	−

Deviation Table

Model	SM1	SM3a(%)	SM3b(%)	SM4(%)	PNM1(%)	MIX1a	MIX1b	MIX2a
					linear finite range models			
H1	7.92	100U	100U	100U	0	−0.81	−2.63	0.41

Conclusions

- The sets of updated constraints (SET2a and SET2b) differed somewhat in the level of restriction but still yielded only 4 and 1 approved RMF models, respectively. A similarly small number of approved Skyrme parameterizations were found in the previous study with Skyrme models. An interesting feature of our analysis has been that the results change dramatically if the constraint on the volume part of the isospin incompressibility ($K_{\tau,\mathrm{v}}$) is eliminated. In this case, we have 35 approved models (SET2a) and 30 (SET2b).

- Our work faces the problematic proliferation of RMF models and our assessment should be used in future applications of RMF models.

- The reasons of many failures, even of the frequently used models, should lead to their improvement and to the identification of possible missing physics not included in present energy density functionals.

This work demanded a huge effort and took 4 years!

Phys. Rev. C 90, 055203 (2014); arXiv:1405.3633[nucl-th]

UFSC

FAPESC

CNPq
Conselho Nacional de Desenvolvimento Científico e Tecnológico

C A P E S

$\boxed{\textbf{Thank you!}}$